

# An Assessment on Silo Design Procedures for Granular Woody Biomass

Diego Barletta, Massimo Poletto

Dipartimento di Ingegneria Industriale, Università di Salerno, Via Ponte Don Melillo, 84084 Fisciano (SA)  
 mpoletto@unisa.it

Particle elasticity and particle fibrous shapes are the main characteristics of biomass and both may be a possible cause of deviation of the biomass behavior from the Coulomb model. In this work we intend to evaluate the possibility to successfully apply the Jenike procedure to the design of storage units containing biomass solids. On this purpose two sawdust samples, a dry one and a humid one, were taken into account. Internal flow properties were characterized by a Schulze ring shear tester while wall friction properties was characterized by a Brookfield Powder Flow Tester. The critical outlet size to allow arch free flow of powder was directly evaluated on a purposely built 0.3 m<sup>3</sup> plane silo. In this silo the wedge shaped hopper allowed to continuously and independently change the hopper angle and the hopper outlet size. Finally, the relationship between the measured flow functions and the arching conditions was assessed by comparing the experimental critical outlet size values with those calculated according to the Jenike design procedure. The results obtained from this comparison indicate that the Jenike procedure is adequate for design purposes with the tested materials. However, it has to be noted that in some cases the difference between the experimental values and the design values of the critical outlet size for an arch free silo is so small to suggest the use of safety coefficients in the application of the design procedure. Furthermore, several biomass particulates, such as those deriving from weeds, straws or canes, may present particle elongation ratios much larger than those of the tested materials and, therefore, the assessment of the flow properties and of the silo design procedure for such materials deserve further studies.

## 1. Introduction

The interest in solid biomass has been increasing over the last decades for their potential as renewable energy sources, to be used in thermochemical processes to produce energy or gaseous fuels (Dai *et al.*, 2008) or biochemical processes to produce liquid fuels like ethanol (Balat, 2008). Solid biomass materials include a wide variety of materials of different natural source. To a first approximation they can be classified in three groups: wood derived biomass, agricultural residues, wet biomass and organic wastes. Usually, biomass is not directly used in conversion processes, but a pre-processing is necessary to obtain granular materials or powders. Industrial practice reports difficulties due to blockage in the discharge from storage units (Mattsson and Kofman, 2002) and difficulties in predicting and controlling biomass flow rates in the feeding of the transformation units (Cummer and Brown, 2002). Solutions to these problems involving special ancillary equipment, that are proposed on empirical basis, increase the handling cost of low value materials so that the economic feasibility of the whole process becomes critical. These problems can be correctly addressed by the knowledge of the flow properties of solid biomass. However, standard characterization methods used for conventional granular solids are not always suitable for biomass materials. The suitability of conventional testers for biomass materials is strongly dependent on the size and the shape of biomass particles. In particular, biomass grinds with particles with more regular shape and small size allow the use of shear cells as tested with woody, flaky and soft materials (Fasina, 2006) recovered fuels (Miccio *et al.*, 2009), very irregularly shaped materials (Owonikoko *et al.*, 2011), woody biomass at high consolidation loads (Miccio *et al.*, 2011) and at low consolidation loads (Miccio *et al.*, 2013). Instead, shear experiments are difficult to perform for biomass materials formed by particles with irregular shapes due to their high compressibility and long strain before the attainment of failure and

steady state stress. Other sources of problems with biomass materials may reside in the design procedures. These procedures (Jenike, 1964) were developed for particulates made of rigid and non-fibrous particles. The simple Mohr Coulomb approach followed in these procedures may be inadequate for materials made of highly elastic particles, such as in the case of lignocellulosic biomass, or made of highly elongated particles, such as in the case of particulates derived from straws or flaky materials. Objective of this paper is to verify the standard design procedures on the flow condition of a plane silo discharging lignocellulosic granular biomass.

## 2. Standard design procedures

The approach due to Jenike (1961), as reported also by Cannavacciuolo et al (2007, 2009), will be followed in this paper. According to it, when the arch is on the verge of collapsing, its weight is just balanced by the vertical component of the maximum normal stress close to the walls. Jenike and Leser (1963) derived the inequality (1) from the force balance on the arch and assuming that the arch is unstable if the material resistance is lower than the abutment stress:

$$f_c < \frac{\rho_b g D}{H(\alpha)} \quad (1)$$

where  $f_c$  is the unconfined yield strength of the powder in use,  $D$  is the effective outlet size,  $\rho_b$  is the powder bulk density,  $g$  is the acceleration due to gravity,  $H(\alpha)$  is a function which takes into account the effects of variation of the thickness of the arch with the silo geometry and the hopper half-angle  $\alpha$ . Jenike and Leser (1963) reported a graphical solution of  $H(\alpha)$  that is well approximated by the following equation (Arnold and McLean, 1976):

$$\frac{1}{H(\alpha)} = \left( \frac{65}{130 + \alpha} \right)^i \left( \frac{200}{200 + \alpha} \right)^{1-i} \quad (2)$$

where the silo geometry is accounted for by the exponent  $i$ ,  $i=0$  for wedge shaped hoppers and  $i=1$  for conical hoppers. In mass flow silos, the consolidation stress at the outlet,  $\sigma_1$ , depends on the distance from the hypothetical hopper vertex. According to Jenike (1961), it is possible to show that:

$$\sigma_1 = \rho_b g D \frac{(1 + \sin \phi_e) s(m, \alpha, \phi_e, \phi_w)}{2 \sin \alpha} \quad (3)$$

where  $s$  is a complicated function depending on the hopper geometry (wedge or conical), on its half angle,  $\alpha$ , on the tensional state ( $m=1$  for active state,  $m=-1$  for passive state), on the powder effective angle of internal friction,  $\phi_e$ , and on the powder wall friction,  $\phi_w$ . Combining the equations (1) and (3) it is possible to obtain the free flow criterion to be applied on the plane  $f_c - \sigma_1$ :

$$f_c < \frac{\sigma_1}{ff} \quad (4)$$

where  $ff$  is the flow factor:

$$ff = H(\alpha) \frac{(1 + \sin \phi_e) s(m, \alpha, \phi_e, \phi_w)}{2 \sin \alpha} \quad (5)$$

Diagrams reporting the flow factors for conical and wedge hopper are given by Jenike (1964) for different values of  $\alpha$ ,  $\phi_e$  and  $\phi_w$ . Flow factors estimates can also be obtained by using the mathematical procedure proposed by Arnold *et al.* (1980). The flow factor line determined by the RHS term of equation (4), generally cuts in two parts the powder flow function  $FF$ , that is the experimental constitutive equation of the material in which the unconfined yield stress  $f_c$  is given as a function of the consolidation stress  $\sigma_1$ :

$$f_c = FF(\sigma_1) \quad (6)$$

According to equation (3), the outlet size  $D$  determining  $\sigma_1$  values on the right of the intersection verify the inequality (4) and, therefore provide solids discharge flow that are arch free. If we call  $f_c^*$  the unconfined yield strength of the material at the intersection between the flow function and the line representing the flow factor, it is possible to calculate the smallest outlet size,  $D_c$ , providing arch free flow by transforming the inequality (1) into an equation and rearranging:

Table 1: Material properties

Materials	$d_{p5}$ [mm]	$d_{p10}$ [mm]	$d_{p50}$ [mm]	$d_{p90}$ [mm]	$\rho_{bp}$ [kg m <sup>-3</sup> ]	$X_w$ %
Wood Powder A	1.11	0.23	0.60	1.30	108	16
Wood Powder B	1.13	0.78	0.95	1.65	112	49

$$D_c = \frac{f_c * H(\alpha)}{\rho_b g} \quad (7)$$

### 3. Experimental apparatus and materials

#### 3.1 Experimental apparatus and procedures

Different shear testers were used to characterize the flow properties of the granular biomass. Namely, the rotational Schulze ring shear tester (RST) was used to measure the internal friction and the material cohesion, the Brookfield Powder Flow Tester was used to measure the wall friction properties. Assuming linear Coulomb yield loci, each yield locus was used to evaluate experimental values of the major principal stress,  $\sigma_1$ , and of the material unconfined yield stress,  $f_c$ . The diagram of the obtained value pairs ( $\sigma_1$ ,  $f_c$ ) provides the material flow function (see for example Tomasetta *et al.*, 2011).

Discharge experiments were carried out in a plane silo (Figure 1), of total volume of about 0.3 m<sup>3</sup>, formed by a parallelepiped bin and a wedge-shaped hopper in which it is possible to independently change both the hopper inclination angle and the width of the outlet slot. Transparent glass front and rear walls of the silo allow the visual inspection of the flowing solids inventory. All the other silo walls are made of stainless steel. The adopted experimental procedure includes: i) the adjustment of the hopper angle and of the outlet slot width; ii) the biomass loading from the silo top while the opening of the hopper is closed by a slab hold by an hydraulic piston; iii) biomass leveling by a rake; iv) a very slow lowering of the closing slab operating on the hydraulic piston and the observation and photo or video recording of the flow regime (flow or arching). For each value of the hopper angle,  $\alpha$ , varied in the range of values ensuring mass flow



Figure 1: Experimental plane silo with variable shape a) sketch; b) full size view; c) material levelling before experiments; d) and e) silo opening; f) stable arch; g) material collected in the discharge basin.

Table 2: Flow properties of biomass powders

Material	$\sigma_1$ [Pa]	$f_c$ [Pa]	$c$ [Pa]	$\varphi_i$ [°]	$\varphi_e$ [°]	$\rho_b$ [kg m <sup>-3</sup> ]	$\varphi_w$ [°]
Wood Powder A	281	54	6	54.7	57.0	127	19
	342	82	14	51.7	56.3	128	
	677	214	42	47.4	54.3	134	
	1401	371	75	46.1	51.9	139	
	2088	600	122	45.6	52.0	142	
Wood Powder B	291	137	51	43.1	69.0	194	25
	582	177	85	40.7	59.0	208	
	1249	370	120	41.4	52.2	220	
	1863	531	156	43.3	52.7	234	

discharge, experiments were repeated with different width of the outlet slot to find the maximum value of the opening,  $D_c$ , that gave rise to the formation of a stable arch.

### 3.2 Materials

Two different woody biomass powders, a dry one (A) made of sawdust sieved below 4mm, and a moist one (B) sieved below 2mm were tested. In this way it was possible to assess also the effect of the material moisture (Landi et al. 2012). Some of the material properties are reported in Table 1. Particle size distributions were measured by sieving. Reported characteristic sizes are the Sauter mean size,  $d_{ps}$ , the 10<sup>th</sup>, 50<sup>th</sup> and 90<sup>th</sup> percentile size,  $d_{p10}$ ,  $d_{p50}$ ,  $d_{p90}$ . Moisture weight fractions in the samples,  $X_w$ , were measured with an Ohaus gravimetric tester. Poured bulk densities,  $\rho_b$ , were evaluated with a graduated cylinder.

## 4. Results

Table 2 reports powders flow properties obtained with the RST, namely the unconfined yield strength,  $f_c$ , the cohesion,  $c$ , the static angle of internal friction,  $\varphi_i$ , the effective angle of internal friction,  $\varphi_e$ , and the bulk density,  $\rho_b$ . The same table also reports the wall friction angle measured with the Brookfield Powder Flow Tester on a coupon cut from the same steel sheet of the silo walls.

Flow function data ( $f_c$  vs.  $\sigma_1$ ) reported in Table 2 and plotted in Figure 2 indicate that according to the

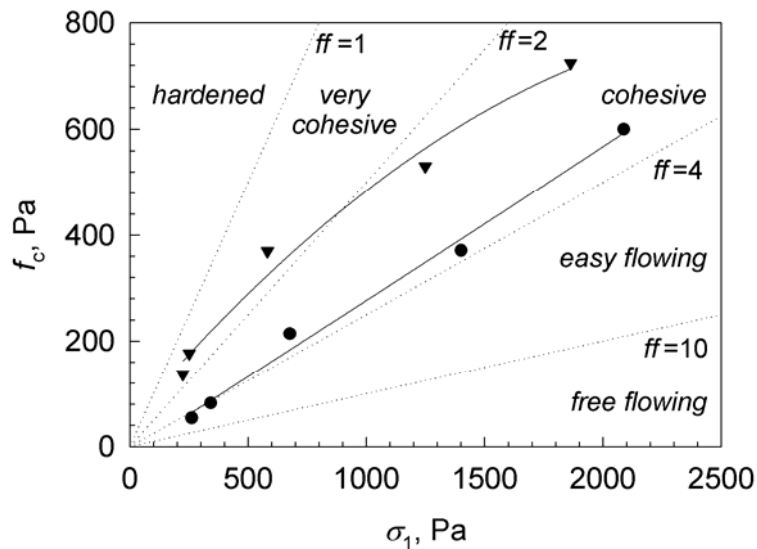


Figure 2: Material flow function (FF) and reference flow factor (ff) lines: ●, Wood Powder A; ▼, Wood Powder B.

Table 3: Main outlet design values

Material	$\alpha$ [°]	$H$ [-]	$ff$ [-]	$f_c^*$ [Pa]	$D_c$ (design) [m]	$D_c$ (exper.) [m]
Wood Powder A	25	1.14	1.17	69.3	0.061	0.04
	26	1.14	1.16	69.3	0.061	0.06
	28	1.16	1.16	69.2	0.062	0.05
	30	1.17	1.16	69.1	0.063	0.07
	32	1.18	1.16	69.1	0.063	0.05
	33	1.18	1.16	69.2	0.064	0.09
Wood Powder B	20	1.11	1.03	329	0.24	0.17
	22	1.12	1.02	328	0.24	0.18
	25	1.14	1.02	327	0.25	0.22
	28	1.16	1.02	327	0.25	0.23
	30	1.17	1.02	328	0.25	0.23

Jenike classification (Jenike, 1964) Wood Powder A falls on the limit between cohesive and easy flowing materials. On the other hand Wood Powder B can be classified as very cohesive or cohesive, depending on the consolidation stress considered.

Results of the silo flow experiments are reported in Figure 3 and in the last column of Table 3, in terms of slot opening  $D_c$ , critical for the arch formation, as a function of the hopper angle  $\alpha$ . In agreement with the above reported classification of the powders according to the flow functions, values of  $D_c$  obtained for the Wood Powder B are larger than those for the Wood Powder A.

According to the design theory presented above, the flow properties reported in Table 2 are used to evaluate design values reported in Table 3. Namely, values of  $H$  functions and flow factors were evaluated according to Arnold and Mc Lean (1976). The intersection between the flow factor  $ff$  lines and the flow functions (FF) determined the critical values of the unconfined yield strength  $f_c^*$ . The latter values were used in equation (7) to determine the theoretical values of  $D_c$ . The comparison between the design and the experimental values of  $D_c$  indicates that the design values somehow overestimate experimental

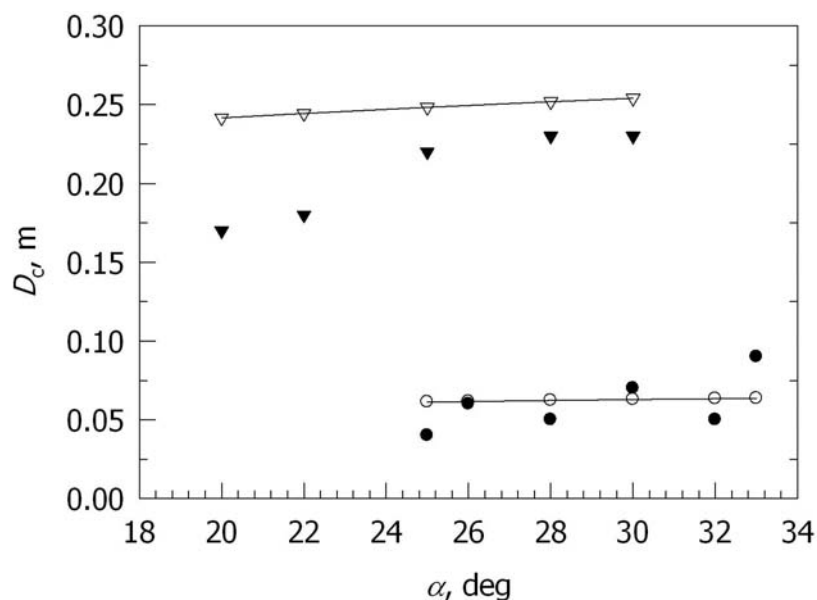


Figure 3: Opening slot width critical to the arch formation,  $D_c$ , reported as a function of the hopper angle. Experiments: ●, Wood Powder A; ▼, Wood Powder B. Jenike (1964) theory: ○, Wood Powder A; ▽, Wood Powder B.

results for the Wood Powder B. Instead design values and experimental values are much closer for the Wood Powder A.

## 5. Conclusions

The equipment and the procedures for measuring the flow properties that are conventionally used in the design of silos resulted suitable also for the application to lignocellulosic biomass powders. The design procedure by Jenike was compared with the experimental data obtained on a pilot scale plane silo with a variable geometry hopper. The design procedure is sufficiently conservative to be used with confidence in the case of damp sawdust Wood Powder B. The same procedure turned out to predict critical outlet values very close to those experimentally found in the case of the dried sawdust Wood Powder B. Therefore, the application of the design procedure in this case requires the adoption of safety coefficients for a reliable hopper design for material flow. Several biomass particulates, such as those deriving from weeds, straws or canes, may present particle elongation ratio much larger than those of the tested materials and, therefore the characterization of the flow properties and the assessment of the silo design procedure for such materials deserve further studies.

## References

- Arnold P.C., McLean A.G., 1976, Improved analytical flow factor for mass-flow hoppers, *Powder Technol.*, 15, 279-281.
- Arnold P.C., McLean A.G., Roberts A.W., 1980, *Bulk Solids: Storage, Flow and Handling*, TUNRA, Newcastle, Australia.
- Balat M., Oz C., 2008, Progress in bioethanol processing, *Progr. Energy Comb. Sci.*, 34, 551-573.
- Cannavacciuolo A., Barletta D., Donsi G., Ferrari G., Schwedes J., Poletto M., 2007, The use of aeration for arch and pipe collapse in the discharge of cohesive powders from a silo, *Chem. Eng. Transactions*, 11, 731-736.
- Cannavacciuolo A., Barletta D., Donsi G., Ferrari G., Poletto M., 2009, Arch-free flow in aerated silo discharge of cohesive powders, *Powder Technol.*, 191, 272-270.
- Cummer K.R., Brown R.C., 2002, Ancillary equipment for biomass gasification, *Biomass Bioen.*, 23, 113-128.
- Dai J., Sokhansanj S., Grace J.R., Bi X., Lim C.J., Melin S., 2008, Overview and some issues related to co-firing biomass and coal, *Canad. J. Chem. Eng.*, 86, 367-386.
- Fasina O.O., 2006, Flow and physical properties of switchgrass, peanut hull, and poultry litter, *Trans. ASABE* 49, 721-728.
- Jenike A.W., 1961, Gravity flow of bulk solids. University of Utah, USA. Utah Engineering Experiment Station, Bulletin 108.
- Jenike A.W., 1964, Storage and flow of solids. University of Utah, USA. Utah Engineering Experiment Station, Bulletin 123.
- Jenike A.W., Leser T., 1963, A flow-no flow criterion in the gravity flow of powders in converging channels. *Proc. 4<sup>th</sup> Int. Congress on Rheology*, 125-140.
- Landi, G., Barletta, D., Lettieri, P., Poletto, M., 2012, Flow properties of moisturized powders in a Couette fluidized bed rheometer, *Int. J. Chem. Reac. Eng.* 10 (1), art. no. A28.
- Mattsson J.E., Kofman P.D., 2002, Method and apparatus for measuring the tendency of solid biofuels to bridge over openings, *Biomass & Bioenergy*, 22, 179-185.
- Miccio F., Landi A., Barletta D., Poletto M., 2009, Preliminary assessment of a simple method for evaluating the flow properties of solid recovered fuels, *Particul. Sci. Technol.*, 27, 139-151.
- Miccio F., Silvestri N., Barletta D., Poletto M., 2011, Characterization of woody biomass flowability, *Chem. Eng. Transactions*, 24, 643-648.
- Miccio F., Barletta D., Poletto M., 2013, Flow properties and arching behavior of biomass particulate solids, *Powder Technol.* 235, 312-321.
- Owonikoko, A., Berry, R.J., Bradley, M.S.A., 2011, The difficulties of handling biomass and waste: Characterisation of extreme shape materials, *Bulk Solids Handling*, 31, 366-371.
- Tomasetta I., Barletta D., Poletto M., 2011, The effect of temperature on flow properties of fine powders, *Chem. Eng. Transactions*, 24, 655-660.